Chem Soc Rev

Cite this: *Chem. Soc. Rev.*, 2011, **40**, 2525–2540

www.rsc.org/csr

CRITICAL REVIEW

Electrolytes for solid-state lithium rechargeable batteries: recent advances and perspectives

Eliana Quartarone and Piercarlo Mustarelli*

Received 16th August 2010
DOI: 10.1039/c0cs00081g

This *critical review* presents an overview of the various classes of Li^+ conductors for use as electrolytes in lithium polymer batteries and all-solid state microbatteries. Initially, we recall the main models for ion transport and the structure–transport relationships at the basis of the observed conductivity behaviours. Emphasis is then placed on the physico-chemical and functional parameters relevant for optimal electrolytes preparation, as well as on the techniques of choice for their evaluation. Finally, the state of the art of polymer and ceramic electrolytes is reported, and the most interesting strategies for the future developments are described (121 references).

A. Introduction

Lithium batteries (LB) are among the power sources of choice for the XXI century energy economy. However, whereas these devices are relatively satisfactory for portable electronics, their performances are far from to be satisfactory for automotive, chiefly in terms of energy and power densities, cyclability, and safety. This makes them very interesting and attractive, both from the point of view of concepts and basic science,[1] and as far as concerns the materials development.[2,3] In fact, about 1500 papers have been published on lithium batteries between January and August 2010.

During the last years, several LB classification schemes were proposed on the basis of the electrodes and electrolyte nature and physical state. However, these classifications are sometimes confusing, and therefore may be useful to reconsider them in a critical fashion. *Lithium battery* (LB) is the common name

Department of Physical Chemistry of the University of Pavia, and IENI-CNR, Via Taramelli 16, 27100 Pavia, Italy. E-mail: piercarlo.mustarelli@unipv.it; Fax: +39 0382 987575; Tel: +39 0382 987205

Eliana Quartarone

Eliana Quartarone received her degree in Chemistry in 1994 and a PhD in Chemical Science in 1999. From 2000 to 2007 she was a post-doc student at the Department of Physical Chemistry of the University of Pavia. She is an assistant professor at the same Department (from 2008). Her research interests are focused on: (i) liquid and polymer ion conducting systems; (ii) proton exchange polymer electrolytes; (iii) thin films based on mixed oxides, for application in optoelectronics, photocatalysis and tissue engineering. She matured experience in the electrochemical and morphological analyses, and in particular impedance spectroscopy and atomic force microscopy.

Piercarlo Mustarelli

Piercarlo Mustarelli got his Master in Applied Physics in 1983, a "Perfezionamento" Degree in Biophysics in 1987, and a PhD in Chemistry in 1992. At present he is Associate Professor of Physical Chemistry at the University of Pavia. He has been visiting scientist at ISI (Brno), ONRI (Osaka) and Warsaw Polytechnical Univ. He is expert of the Italian Ministry of Industry for industrial projects evaluation. During the last five years he obtained grants for more than 2 million Euros. He authored or co-authored about 150 publications on international journals, more than 250 contributions at international or national conferences, and 2 patents. Mustarelli's research interests span from the development on NMR instrumentation, to the study of electrolytes and electrodes for lithium batteries and fuel cells, to (nano)biomaterials.

given to primary (disposable) devices having lithium metal or a lithium compound as the anode. *Lithium ion battery* (LIB) indicates a family of secondary (rechargeable) devices where both the electrodes are intercalation materials, and the electrolyte is a lithium salt dissolved in a mixture of organic solvents. *Lithium polymer battery*, or alternatively, *lithium-ion polymer battery* (LPB, LIPB) is a rechargeable device where the lithium salt is somehow entrapped in a polymer (or composite) membrane. The anode may be Li metal or a Li-based intercalation compound, and the cathode is an intercalation oxide. *Lithium air battery* (LAB) is a device where a lithium anode is electrochemically coupled with the atmosphere through a ceramic composite cathode, the electrolyte being liquid or polymer-based. The main advantage of this device is given by its very high specific energy, 11 140 Wh kg^{-1} (excluding oxygen), which is not far from that of the gasoline/air engine (11 860 Wh kg^{-1}). Finally, *lithium microbattery* (LM) is an all-solid-state thin film device, where the anode may be Li metal or an intercalation compound, the cathode is an intercalation compound, and the electrolyte is a glassy, glass–ceramic or ceramic Li^+ conductor. The layers can be deposited by means of the physical vapour deposition (PVD) or chemical vapour deposition (CVD) method. Fig. 1 shows the Ragone plot of some primary (disposable) and secondary (rechargeable) batteries. At present, Li–air devices may offer the best performances in terms of energy density, although the attainable power density levels are not yet fully satisfactory.

Inside the battery, the electrodes (mainly the cathode) are the limiting factors in terms of overall capacity, *i.e.* energy density, and cyclability. The electrolyte, on the other hand, does determine the current (power) density, the time stability, and the safety of the battery. However, while the electrodes have been the objects of extended reviewing,[4–7] only a limited attention has been devoted to the electrolytes.[6] In particular, most reviews are outdated,[8,9] while a recent work discusses polymer electrolytes in the frame of a more general overview.[10] New concepts and materials have emerged in the field, chiefly regarding materials processability, battery safety and environmental impact.

In the following the attention will then be focused on the electrolyte. Again, different classification schemes were proposed during the past decades. The most detailed scheme is due to Jacob *et al.*,[11] who divided polymer electrolytes into five classes: (1) polymer/salt complexes (*e.g.* PEO–$LiClO_4$); (2) plasticized electrolytes, where a (small) liquid amount (*e.g.* propylene carbonate, PC) is added to "class 1" complexes; (3) gel electrolytes, formed by incorporating an organic electrolyte solution into a polymer matrix (*e.g.* PVDF/$LiPF_6$–EC–PC); (4) polymer-in-salt (or rubbery) electrolytes, where the polymer fraction is a minority with respect to the salt;[12] (5) (nano)composite electrolytes, where ceramic fillers are added to a polymer electrolyte. In this review we will chiefly concentrate our attention on lithium polymer electrolytes, by adopting a more concise scheme: (1) solid polymer electrolytes (SPEs), and (2) gel polymer electrolytes (GPEs). Our first class will embrace (1) and (5) groups of Jacob *et al.*, whereas GPEs will collect (2) and (3). The polymer-in-salt concept has not yet led to significant technological developments. Besides the polymer electrolytes, a specific section will be also devoted to thin film glassy, glass–ceramic and ceramic electrolytes for lithium microbatteries.

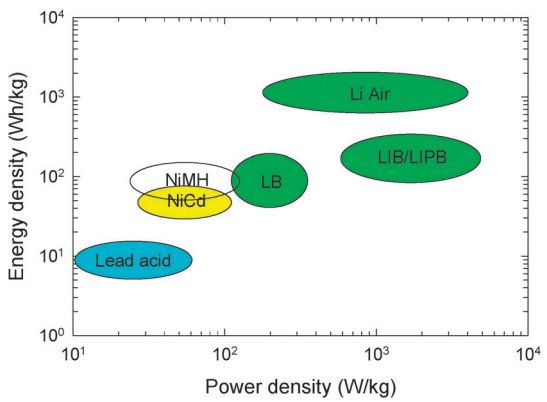

Fig. 1 Ragone plot of some primary and secondary batteries.

B. Models for ion transport

A comprehensive physical description of ion transport in polymer electrolytes cannot be easily obtained because of the large variety of systems involved, and of the lack of simple structure–properties correlations. Generally speaking, the ionic conductivity of these systems can be modelled in terms of Arrhenius or Vogel–Tammann–Fulcher (VTF) behaviours, or of a combination of both of them.[13,14]

The Arrhenius behaviour of the ionic conductivity, σ, is described by eqn (1)

$$\sigma = \sigma_0 \exp\left(\frac{-E_a}{kT}\right) \quad (1)$$

where the pre-exponential factor σ_0 is related to the number of charge carriers, and the activation energy for conductivity, E_a, may be computed from the linear best-fit of $\log \sigma$ *vs.* $1/T$ plots. The other symbols have the usual meaning. The Arrhenius behaviour is generally related to ion hopping decoupled from long-range motions of the matrix (*e.g.* amorphous polymer and glass phases below the glass transition, ceramic ion conductors, *etc.*).

The VTF behaviour, which is more relevant for polymer electrolytes, is described by eqn (2)

$$\sigma = \sigma_0 T^{-\frac{1}{2}} \exp\left(-\frac{B}{T - T_0}\right) \quad (2)$$

Here B is the pseudo-activation energy for the conductivity (expressed in units of E_a/k), and T_0 is the reference temperature which normally falls 10–50 K below the experimental (kinetic) glass transition, T_g. The VTF parameters can be obtained by fitting the conductivity data in terms of the linearised relationship (3)

$$\log_{10}(\sigma T^{\frac{1}{2}}) = \log_{10}\sigma_0 - 0.43\frac{E_a}{k(T - T_0)} \quad (3)$$

where T_0 is treated as a parameter. Alternatively, a three-parameter, non-linear best-fit can be used. The VTF equation may be derived by quasi-thermodynamic models like free volume[15] and configurational entropy,[16] and its behaviour is related to ion motion coupled with long range motions of the

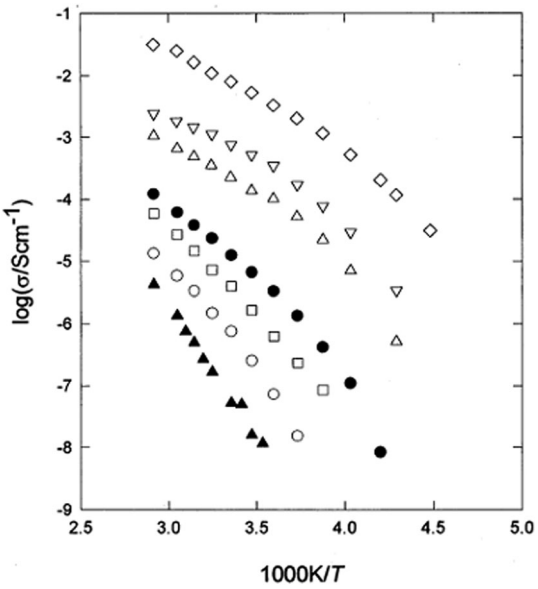

Fig. 2 Conductivity plots for the gel electrolytes P(VDF–HFP) activated with 1 M EC/DEC/LiN(CF_3SO_2)$_2$ solution. Polymer/solution weight ratios: ▲ 80 : 20; ○ 70 : 30; □ 60 : 40; ● 50 : 50; △ 40 : 60; ▽ 30 : 70; ◇ 20 : 80. Reprinted from ref. 17.

polymer branches and/or solvent molecules. VTF behaviours are generally observed in: (i) SPEs above the T_g of the polymer matrix, (ii) GPEs,[17] (iii) electrolyte organic solutions, (iv) ionic liquids.[18] Some typical VTF behaviours are reported in Fig. 2.

A specific treatment is necessary for nanocomposites, which have gained large interest in the last years.[19] These materials are obtained by distributing a second (in such cases even a third) phase, with particles of nanometric dimension, in a matrix that can be amorphous or crystalline. The additives (fillers) can be classified as active or passive from the point of view of the conductivity. Active fillers contain moieties which can contribute to the conduction (*e.g.* γ-$LiAlO_2$),[20] and give origin to complex conductivity behaviours *vs.* their weight content. The addition of a passive filler (Al_2O_3, SiO_2, TiO_2, *etc.*) can determine a conductivity increase even larger than one order of magnitude, that may be associated with Lewis acid–base interactions among the surface of the ceramic nanoparticles, the polymer chains and the lithium salt,[21] or to grain boundary effects, *e.g.* to the formation of a space–charge layer at the electrolyte/filler interface.[22]

The behaviour of the ionic conductivity *vs.* the passive filler content is normally non-linear with a maximum in the range 5–15 wt% of filler, depending on the polymer matrix, the lithium salt and the filler nature. A typical behaviour is reported in Fig. 3.

The conductivity of composite materials made by a conducting and an insulating phase may be described, in principle, by effective media theories,[23] which may also be applied to dielectric and magnetic properties, thermal conductivity, and diffusion coefficients. Most aspects of general percolation and effective media theories were combined to give the General Effective Medium (GEM) equation[24]

$$\frac{f(\sigma_1^{1/t}-\sigma_m^{1/t})}{\sigma_1^{1/t}+A\sigma_m^{1/t}}+\frac{(1-f)(\sigma_2^{1/t}-\sigma_m^{1/t})}{\sigma_2^{1/t}+A\sigma_m^{1/t}}=0 \qquad (4)$$

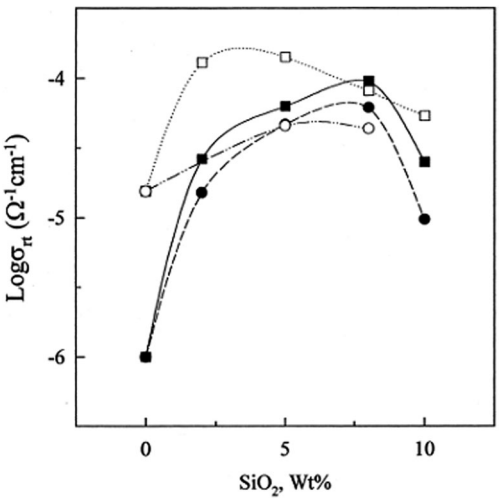

Fig. 3 Conductivity values at room temperature *vs.* the filler (nanosize SiO_2) content. ■: PEO_8–$LiClO_4$ with SiO_2 treated at 900 °C; ●: PEO_8–$LiClO_4$ with SiO_2 treated at 100 °C; □: PEO_8–LiN(CF_3SO_2)$_2$ with SiO_2 treated at 900 °C;: PEO_8–LiN(CF_3SO_2)$_2$ with SiO_2 treated at 100 °C. Reprinted from ref. 22.

where σ_1, σ_2 and σ_m are the conductivities of the two phases and of the composite material, respectively, the constant A depends on the particular composite medium and the approach to the problem, and the exponent t is related to the filler volume fraction f, and to the grains shape.

C. Key parameters in electrolyte optimization

In this section we will critically discuss the most important physico-chemical parameters—besides the ionic conductivity—to be considered in electrolyte optimization, and the experimental techniques of choice for their investigation. Emphasis will be given, when possible, to the *in situ* approaches which are becoming increasingly important. The discussion will chiefly consider polymer electrolytes, although the majority of concepts are also suitable for ceramics and glass–ceramics.

Thermal properties and chemical stability

The thermal parameters generally considered in the optimization of an electrolyte are the glass transition temperature, T_g, the melting point, T_m and, if the case, other phase transitions temperatures. The degree of crystallinity is another parameter of interest which can be obtained from thermal analysis. Degradation phenomena must be also investigated to evaluate the thermal stability of a material and its capability to work in the operative temperature range of a lithium battery (from −50 °C to 80°C for military applications). The thermal analysis of the electrolytes is normally carried out by means of: (i) differential scanning calorimetry (DSC)[25] and (ii) thermogravimetry (TGA).[26] The DSC measures the differential heat flow between a sample and an inert reference material. It works between sub-ambient temperatures (around −150 °C) and about 800 °C. It is usually employed to determine the heat of a transition and the heat capacity. TGA is an analytical technique used to determine the thermal stability of the materials. Both inert and reactive gaseous atmospheres may

be used, namely N_2, Ar, air, and O_2, the last two being useful to investigate oxidative processes. In the case of polymer electrolytes, the analysis is normally performed between the room temperature and 600–800 °C, at heating rates typically lying in the range 2–10 °C min^{-1}. Modern TGAs work in a "high resolution mode", which means that the heating rate is dynamically increased (or reduced) to properly follow fast (or slow) processes. The thermogram, which monitors the weight loss occurring when the sample is heated, provides: (i) the sample residual mass, and (ii) the decomposition or oxidation temperatures.

Ion transport number

Transport (or transference) number, t^i, of a given ion is defined as the fraction of the total current carried through the electrolyte by this particular anion, with the convention that $\sum_i t^i = 1$. In the case of a single salt of monovalent ions, the following relationship holds

$$t^{\pm} = \frac{\mu_{\pm}}{\mu_+ + \mu_-} \qquad (5)$$

where $\mu_{\pm}$ are the mobilities of the cation and the anion, respectively. Transport numbers have been determined by several methods, including Hittorf,[27] moving boundaries, and radiotracers. However, the Hittorf method does require a three-compartment cell which must be disassembled after the experiment, and can be hardly applied to the study of solid (or gel) polymer electrolytes. Recently, the t^+ values of SPEs and GPEs have been generally determined by means of dc polarization combined with impedance spectroscopy, as proposed by Bruce *et al.* (ac/dc method).[28] The method consists of applying a small dc pulse, ΔV, to a symmetrical Li|electrolyte|Li cell and measuring the initial, I_0, and the steady-state, I_{ss}, current which flow through the cell. The same cell is also monitored by impedance spectroscopy to detect the initial, R_0, and the final, R_{ss}, resistance of the two Li interfaces, to account for the resistance of passivation layers and the eventual increase of this value upon the duration of the dc pulse. Under these circumstances, the lithium transport number, t^+, is given by

$$t^+ = \frac{I_{ss}}{I_0}\frac{\Delta V - I_0 R_0}{\Delta V - I_{ss} R_{ss}} \qquad (6)$$

This method is valid for the electrochemical systems in which the charge transfer reaction is not the limiting step in the cell.[28] Indeed, this may be not the case of some systems and components of increasing interest for lithium batteries, *e.g.* ionic liquids. The problem may be overcome by a proper choice of the polarization voltages, which must be increased in order to balance the *iR* drops due to the larger resistances of the passivation layers on the lithium electrode, as thoroughly discussed by Abraham and co-workers for both liquid and polymer electrolytes.[29] The ac/dc method works well in the case of highly dissociated salts, but is not able to discriminate between single ions and charged triplets.

The cation transport number can be easily determined by Pulse Magnetic Field Gradient (PMFG) NMR if both the anion and the cation self-diffusion coefficients can be measured. This is indeed the case of lithium fluorinated salts

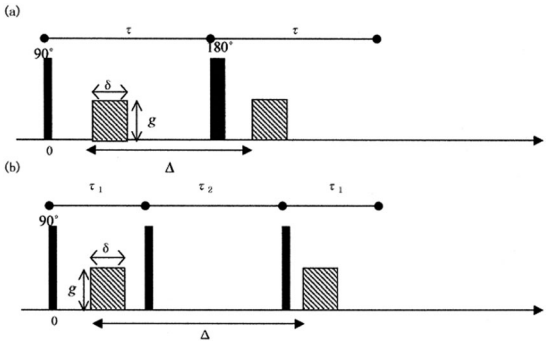

Fig. 4 PMFG NMR sequence (part a); SPFG NMR sequence (part b). Reprinted from ref. 31.

($LiBF_4$, $LiPF_6$, $LiN(CF_3SO_3)_2$, *etc.*) which are commonly employed in SPEs and GPEs. Here the transport number is given by

$$t^+ = \frac{D_{Li}}{D_{Li} + D_F} \qquad (7)$$

where D_{Li} and D_F are the self-diffusion coefficients of lithium and fluorine, respectively. This approach was earlier applied by Clericuzio *et al.* to plasticized polymer electrolytes.[30] A variation of the method (Stimulated Pulse Field Gradient, SPFG) was lately applied by Saito *et al.* to PVDF-based GPEs.[31] The NMR sequences of the two approaches are reported in Fig. 4.

With both the sequences the self-diffusion coefficient, D, is obtained by a linear best-fit of the relation giving the spin-echo intensity, M

$$M = M_0 \exp\left[-D(\gamma G\delta)^2\left(\Delta - \frac{1}{3}\delta\right)\right] \qquad (8)$$

where M_0 is the initial spin-echo value, γ is the gyromagnetic ratio, g and δ are the strength and the duration of the magnetic gradient pulses, respectively, and Δ is the separation time between the two gradient pulses. The main limitations of this NMR approach are: (i) the need of strong electric current boosters and efficient coils to generate the high electromagnetic gradients required to measure solid-state diffusion coefficients often less than 10^{-11} m^2 s^{-1}; (ii) the impossibility to separate the contributions of single ions and ion pairs. A solution for the last problem is offered by electrophoretic NMR, where the mobility of the nuclei is determined by a stimulated echo experiment with a synchronized electric field pulse.[32]

Electrochemical stability

Besides the ionic conductivity, other electrochemical parameters must be considered in the design of new materials for lithium batteries. The electrolyte, in fact, should have a good ionic conductivity (at least of the order of 1 mS cm^{-1} at room temperature), and also a good electrochemical stability and compatibility with the electrodes. The electrochemical stability is evaluated by considering several parameters, namely the Li/electrolyte interfacial resistance, the electrochemical window and the electrolyte behaviour during battery cycling tests.

When the electrolyte is put in contact with Li metal, a solid electrochemical interface (SEI) is formed. The interfacial resistance is the physical parameter describing the evolution of the passivation layer. The interface behaviour is evaluated by following the time evolution of the overall resistance of a symmetrical Li|electrolyte|Li cell. In principle, Impedance Spectroscopy (IS) is the most powerful tool to measure the complex impedance, Z.[33] The technique is based on the application of an ac voltage in the (typical) frequency range 10 MHz–1 mHz, and on the measurement of the resulting electric current. The interfacial resistance is obtained from a complex plot of the imaginary part of the impedance, Z'', *vs.* the real part, Z' (Nyquist plot). This plot allows to separate the resistive contributes related to the bulk, grain boundary and interfacial resistances, and provides also capacitive information. The electrode/electrolyte interface behaves like a parallel resistance–capacitance circuit (RC), described by a semicircle in the Z plane. Fig. 5 shows, as an example, the time evolution of the interfacial resistance and the relative impedance spectra of two Li cells based on an unfilled PVDF-based gel electrolyte and a composite one.[34]

The intercept at high frequency (see Fig. 5 inset) on the Z real axis is the electrolyte resistance. In addition, the diameter of the semicircle gives the overall interfacial resistance, which takes into account the resistance of the charge transfer through the interface and that one associated to the growth of a passivation layer on the lithium anode. After an initial instability, the interfacial resistance, R_i, does increase due to the formation of passivation layers on the lithium surface. However, in the case of the SBA-based membrane, R_i quickly reaches a stability plateau, around 150 Ω cm^{-2}, whereas it continuously grows with time in the unfilled gel. Both the structure and the chemical composition of the interface are important aspects to know to understand the electrolyte electrochemical behaviour. Recently, *in situ* spectroscopic experiments were carried out in order to investigate the surface chemistry of reactive electrodes. Chusid *et al.* used *in situ* FTIR for describing the interface in Li|electrolyte|Li cells.[35] Two systems were investigated, PVDF-based gel electrolytes, plasticised with organic carbonates, and solvent-free branched PEO–salt complexes. The authors demonstrated that in the case of the gel electrolytes, the Li surface in contact with the carbonate solution is covered by the products coming from the solvent reduction to $ROCO_2Li$. In contrast, in the case of dry polymers, the passivation layer is substantially constituted by a mixture of water and lithium salts. The electrode surface can be also studied from a morphological point of view. In 2004, Cohen and Aurbach used *in situ* AFM imaging on Li/V_2O_5 microbatteries with liquid electrolytes.[36] In this case the grain growth and the detrimental effect of the salt anion on the electrochemical intercalation performances were investigated by considering two different lithium salts, namely $LiPF_6$ and $LiClO_4$.

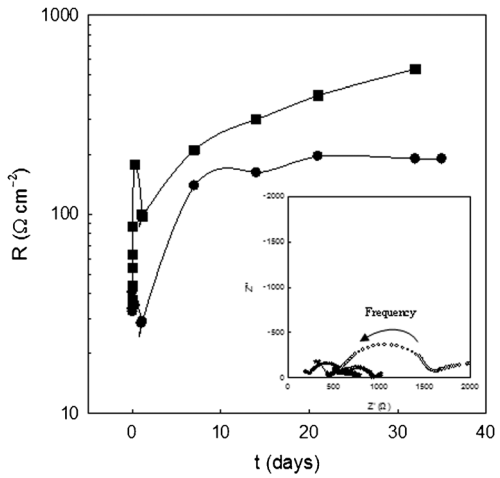

Fig. 5 Evolution of the interfacial resistance at room temperature in a Li/Li$^+$ cell with an unfilled PVDF–HFP membrane (filled squares) and a composite gel electrolyte containing 10 wt% of mesoporous silica SBA-15 (filled circles). The inset shows the impedance spectra of the unfilled gel (circles) and of the composite electrolyte (stars) after 7 days (filled symbols) and 30 days (open symbols). Reprinted from ref. 34.

Impedance spectroscopy may be also used during the charge–discharge battery tests, in order to perform an *in situ* investigation of the interfacial resistance with the cathode. Recently, Zaghib and coworkers performed some experiments of stepwise IS on Li/IL-based gel electrolytes/$LiFePO_4$ at different states of charge.[37] This technique revealed that a stable interfacial resistance is obtained only when the cathode reaches 70% of depth of discharge. Further, the diffusion resistance values were measured, which resulted to be higher in the presence of single-phase olivine.

The electrochemical stability of the electrolyte is also evaluated by estimating the reduction and oxidation potential limits with respect to a defined couple of electrodes. In particular, the reductive breakdown of the salt anion or solvent is an important phenomenon which affects the formation of the passivation layer at the interface. The potential window is measured by sweeps of linear or cyclic voltammetry. In principle, a standard cell configuration for these experiments consists of a three-electrode system where Li is used both as a counter electrode and reference, whereas a metal like Ni or Cu as the working one. Fig. 6 shows the anodic voltammetry scans for a PVDF-based gel electrolyte activated with a solution of an ionic liquid ($PYR_{1,2O1}$-TFSI, see following) doped with LiTFSI, and for the homologue composites filled with SBA-15 and HiSil T700™.[34] The onset voltage is associated to the anodic decomposition limit of the electrochemical stability window. This limit is higher in the case of composite gels (about 4.0 V). Both the fillers improve the electrochemical stability of the membranes, but the best performances are obtained with SBA-15. As we will discuss in details in the next section, the positive effects of the mesoporous filler in terms of interface stability are likely related to its hierarchical microstructure, which allows a more homogeneous particle distribution through the matrix with a consequent larger polymer/filler interface.

The decomposition phenomena of the electrolytes and the electrochemical stability windows (EW) are often complicated to interpret. This is particularly true when ionic liquids are used as part of the electrolyte, since their electrochemical properties are strongly affected by the combination of an anion and a cation, and they do react with metallic lithium.

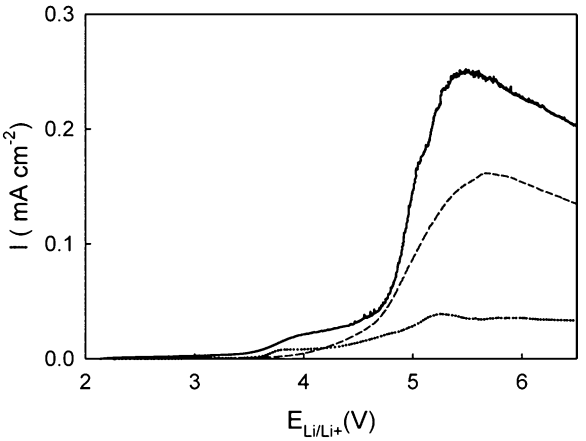

Fig. 6 Linear voltammetry plots *vs.* Li/Li^+ of some gel electrolytes: unfilled PVDF-based membrane (solid line); the same with 5 wt% of HiSil™ (dashed line); the same with 10 wt% of SBA-15 (dotted line). Scan rate: 5 mV s^{-1}. Reprinted with modifications from ref. 34.

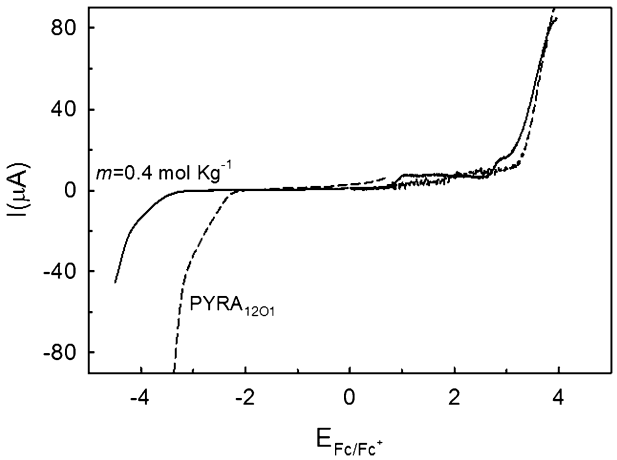

Fig. 7 Linear voltammetry plots of the $PYR_{1,2O1}$-TFSI ionic liquid (dashed line), and $PYR_{1,2O1}$TFSI–LiTFSI solution (m = 0.41 mol kg^{-1}) (solid line) *vs.* Fc/Fc^+. Scan rate: 10 mV s^{-1}. Reprinted from ref. 34.

In this case, materials other than lithium can/must be used. As a consequence, the comparison of the data from different authors is difficult, since the reference systems are different and, sometimes, not strictly electrochemically defined. Therefore, as also recommended by IUPAC, it is necessary to develop potential scale reference systems. This scale can be set up by using a reference electrode of known potential against a standard reference electrode and also by referencing all data to a process with reversible potential independent of the ionic liquid.[38] The ferrocene/ferrocinium, Fc/Fc^+, couple is an ideal and commonly used internal potential-scale standard in the case of not highly viscous ionic liquids. Ferrocene undergoes a reversible oxidation process involving one electron:

$$Fc(IL) \leftrightarrows Fc^+(IL) + e^- \quad (9)$$

Fig. 7 reports, as an example, the linear voltammetry of a PYR_{12O1}TFSI–LiTFSI system, and of the pure ionic liquid.[34] The electrochemical data were obtained using an Ag^+/Ag reference electrode, calibrated to the ferrocene–ferrocinium redox couple in order to obtain an absolute reference. By comparing the two plots, we see that the solution is electrochemically more stable than the pure ionic liquid. Its stability window is 5.8 V, ranging from −3.3 to 2.5 V *vs.* Fc/Fc^+, whereas $PYR_{1,2O1}$-TFSI has a significantly smaller window of 4.9 V (from −2.2 to 2.7 V *vs.* Fc/Fc^+). The difference in the cathodic stability (−3.3 V for the solution and −2.2 V for the liquid) is probably related to the presence of a higher amount of the $TFSI^-$ anion coming from the dissolved salt. It is known from the literature that the reduction limit of this anion in pyrrolidinium-based structures causes decomposition processes, leading to the formation of a protective passivation layer on the working electrode which somehow prevents the reduction of the cation. Further, the higher potential necessary to decompose the anion, observed in the case of Li-doped ionic liquid, may be also due to the strong coordination between Li^+ and $TFSI^-$.[39] Finally, it should be considered that the EWs should be also determined by using lithium metal, in order to have a first indication of the problems the electrolyte can meet under operating conditions.

Battery tests

In order to evaluate the suitability of a given electrolyte to work in a lithium battery, anode(Li)/electrolyte/cathode cells must be assembled and cycled in a proper voltage range, depending on the selected electrodes. The cycling behaviour is investigated by changing temperature, current density and discharge (C) rates. C1 (C = 1) rate means that the cell is completely discharged within one hour. C/10 (C = 0.1) indicates that the full discharge takes place in 10 hours. The voltage profiles with time are then used to calculate (i) the specific capacity, normally expressed in milliampere hours per gram, mA h g^{-1}, delivered during the cell charge and discharge, and (ii) the charging/discharging efficiency. In principle, the role played by the electrolyte in determining the cell performances is correlated to the passivation layer formed at the interface with the Li surface. High internal cell resistances, in fact, cause abrupt falls in the capacity values and, consequently, degradation of the capacity during cycling. As an example of the problems which can be disclosed by proper battery tests, Fig. 8 reports the charge and discharge behaviours of a solid

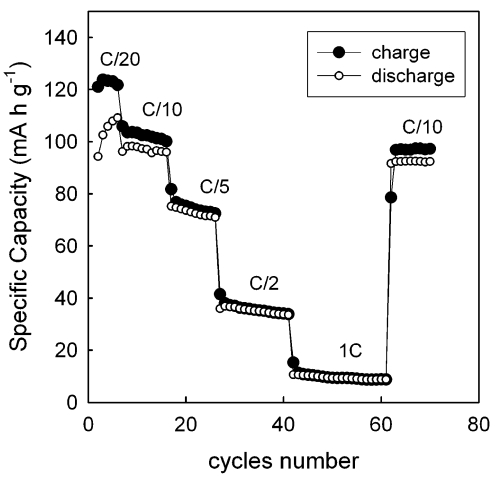

Fig. 8 Cycling behaviour of a solid state cell Li/PEO_{20}–LiTFSI–$PYR_{1,2O1}$TFSI/$LiFePO_4$ at room temperature. Unpublished results.

state cell Li/PEO–LiTFSI–$PYR_{1,2O1}$TFSI/$LiFePO_4$ at room temperature. The hysteresis observed at low C rates is the demonstration of poor electrolyte stability (likely due to decomposition), whereas the very low capacity and the strong decays at the highest current regimes (C/2, 1C) are an indication of concentration polarization (increasing value of the interfacial resistance), likely underlying a low Li^+ transport number. Similar correlations between the unstable plateau of the capacity and high interfacial resistance were found for instance by Passerini *et al.* in other PEO–LiTFSI electrolytes plasticised with PYR-based ionic liquids.[40]

D. State of the art and recent trends

As stated in the Introduction, the electrolyte is actually the main component determining the current (power) density, the time stability, and the safety of the battery. Taking into account that the electrolyte is in intimate contact with the electrodic compartments, a good chemical and physical compatibility with both the electrodes is required in order to obtain a stable electrified interface (EI) and, consequently, energy and power density values stabilised with time. In the particular case of LIB, the electrolyte consists of organic solutions based on lithium salts dissolved in polar and aprotic carbonates. In spite of a wide variety of liquid electrolytes developed during the 1990s, many LIB preferentially use some optimised formulations, which consist of proper concentrations of $LiPF_6$ in a mixture of ethylene carbonate (EC) and a linear alkyl carbonate. The success of this specific formulation is due to several reasons: (i) high dielectric constant of the cyclic carbonates, and in particular of EC, which allows to dissolve lithium salts even at high concentration (up to 1.0 M); (ii) low viscosity of the linear carbonates; (iii) a consequent good ionic conductivity (higher than 1 mS cm^{-1} at room temperature); (iv) low melting point of the solution. A detailed summary on the explored lithium salts and solvents was reported a few years ago.[41]

The liquid electrolyte is absorbed on a separator, namely a porous membrane which does not hinder the ionic flow and protects from short circuits. The separator plays an important role on the overall performance of a lithium battery, and several materials were investigated in the recent past, also in order to state how membrane parameters like thickness, morphology, pore microstructure, chemical and mechanical stability and retention capability may affect the cell electrochemistry. At present, the most common separators are microporous films of polypropylene or polyethylene, which are electrochemically stable in primary and secondary Li batteries, respectively.[42] However, inorganic composite membranes, made of porous matrices coated on both sides by nano-sized materials, seem to better answer to both safety and dimensional stability requirements even at higher temperatures.[43] In spite of some promising physico-chemical properties, the carbonate-based liquid electrolytes may undergo deterioration, with consequent safety problems, related to irreversible reactions with the electrodes. These processes generally lead to the formation of dendrites, exfoliation or degradation, in particular of the anode, with a large irreversible capacity loss. Furthermore, the decomposition phenomena may be highly exothermal, and the evolution of gaseous by-products, which may cause abrupt pressure increases and consequent explosion of the device, is not rare. In order to inhibit the electrode corrosion and to form a stable solid electrified interface (SEI), many additives were recently tested, which may also act as flame retardants. They include catechol carbonate, alkyl sulfones, alkyl phosphates or phosphazenes.[44–47] It must also be considered that liquid electrolytes require the sealing of the battery and, generally speaking, a more complex cell management.

Because of these problems, during the last two decades the attention of academy and industry has been focused on the search for alternative electrolytes for lithium batteries. One of the most followed approaches is the fabrication of all solid-state batteries. The main reason to use a solid material is that the problems related to the management of a liquid medium are overcome. In the following we will discuss both polymer electrolytes (SPEs and GPEs), and ceramic and glass–ceramic electrolytes. The former class is well suited to fabricate cells in portable devices and/or in the automotive field. Ceramic (and glass–ceramic) materials are generally used as thin film electrolytes in microbatteries, chiefly because of the suitability as target materials in deposition technology, which counterbalances their lower ionic conductivity.

In principle, polymer-based electrolytes for lithium batteries must satisfy some basic requirements: (i) ionic conductivity higher than 10^{-4} S cm^{-1} at room temperature, (ii) good thermal, chemical and mechanical stability, (iii) a lithium transport number close to unity, (iv) compatibility with the electrodes (wide electrochemical windows). The first study on ion conducting polymers was proposed by Fenton *et al.* in 1973,[48] and was concerned with polyethylene oxide-based complexes with several alkaline salts. After that, a number of possible systems was described in the literature, and many polymers and co-polymers were tested as potential electrolytes for PLB.[9,10,14] Polymers with ether-based groups, like polyethylene oxide (PEO), polypropyleneoxide (PPO) and their copolymers, or more inert (cage) matrices, for instance polyvinylidene fluoride (PVDF) and its copolymers with hexafluoropropylene [P(VDF–HFP)], polyacrylonitrile (PAN) and polymethyl-methacrylate (PMMA), were selected for their promising performances. In spite of such a large variety of polymers, PEO and PVDF-based matrices are still the best choice to prepare SPEs and GPEs, respectively. Here we will firstly recall the most recent novelties in the polymer electrolytes development, and namely: (i) the use of new lithium salts, and (ii) the use of ionic liquids as media for the lithium-based solutions. Then we will discuss their applications in polymers, which give origin to the ''new generation'' solid state electrolytes. A paragraph devoted to the thin film electrolytes for microbatteries will conclude this Section.

New high-performance lithium salts

The lithium salts used in lithium batteries are characterized by a big superacid anion, *i.e.* a structure where the negative charge is well delocalised in the presence of withdrawing ligands with Lewis acid properties. The more commonly investigated salts are $LiPF_6$, $LiBF_4$, $LiN(CF_3SO_2)_3$, $LiClO_4$,

$LiAsF_6$, $LiCF_3SO_3$, *etc*. However, as already stated, the most used salt in the commercial liquid electrolytes is indeed $LiPF_6$. The reason for such a success depends on several factors. First, when dissolved in alkyl carbonates, $LiPF_6$ shows high conductivity, which may exceed 10 mS cm^{-1} at room temperature, and it also shows good solubility properties in various solvents. Further, its oxidation stability reaches $\sim$5 V, and the PF_6^- anion easily forms a passivation layer on an Al substrate at high potentials. On the other hand, its thermal instability and hygroscopicity are well known. The salt easily decomposes in LiF and gaseous PF_5 and, in the presence of small traces of moisture, the P–F bonds also undergo hydrolysis then developing corrosive gaseous by-products. We followed the degradation process of $LiPF_6$ in a PEO_x–salt system by means of ^{31}P solid-state NMR. In particular, we showed that the salt decomposes to give LiF and different fluorophosphates-based products, depending on the moisture level.[26]

About ten years ago, Barthel *et al*. proposed new lithium salts containing a chelated boron anion, with promising physical and electrochemical properties.[49] The first proposed chelating agents were aromatic ligands, such as benzene (LBBB)-, naphthalene-(LBNN), or diphenyl-diolato (LBBPB) systems, which show very high thermal stability, at least under low moisture conditions.[41,49] The main feature of these salts is the huge charge delocalization due to the presence of highly withdrawing substituents on aromatic rings, which allows quite high oxidation potentials (up to 4.5 V). The strong correlation between the electrochemical stability and the HOMO energies was quantified through *ab initio* calculations.[41,50] However, the presence of aromatic units limits the solubility of such salts, which leads to relatively low conductivity. Values in the range 0.6–11 mS cm^{-1} were observed, depending on the used solvents. In order to overcome the solubility problems, and to improve both conductivity and electrochemical stability, a new series of borate salts was proposed where the borate anion is constituted by an alkyl-based bidentate ligand.[41,51] Also in this case there is a large electron withdrawing effect due to the presence of fluorine or/and carbonyl groups. The use of less bulky substituents favours the salt dissociation in the common solvents used for lithium batteries. Consequently, higher conductivity values, only slightly lower than those of the conventional liquid electrolytes, were obtained. One of the most studied boron-based salt is lithium bis(oxalato)borate, $LiB(C_2O_4)_2$ (LiBOB) (see Scheme 1), which shows several advantages when dissolved in alkyl carbonates: (i) it is more thermally stable and environmentally safer than $LiPF_6$, and (ii) it forms a stable solid electrolyte interface on the lithiated graphite, so remarkably improving the reversibility of the negative electrode.

For this reason LiBOB was also used as the salt in propylene carbonate (PC)-based solutions, in order to overcome the Li cointercalation of PC molecules in the graphite with consequent electrode exfoliation. Stable capacity and coulombic efficiency close to unity were obtained at least for 80–90 cycles.[52] However, lithium oxalate borate shows lower ionic conductivity (about 7 mS cm^{-1} at rt) and worse performances at low temperatures with respect to $LiPF_6$-based solutions. Therefore, borate salts were tested also as additives in the conventional liquid electrolytes to increase the performances towards the graphite anode.[53]

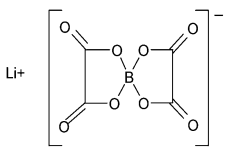

Scheme 1 Chemical structure of lithium bis(oxalato)borate, LiBOB.

More recently, new fluorinated boron-based salts with expected outstanding properties have been proposed including, for example, pentafluorophenyl boron oxalate (PFPBO),[54] and polyfluorinated boron cluster lithium salts ($Li_2B_{12}F_xH_{12-x}$).[55]

Ionic liquids

Ionic liquids (ILs) are salts which melt near or below room temperature. In particular, those salts which are liquid at rt are named "Room Temperature Ionic Liquids" (RTILs). They have recently been attracting a growing attention from the scientific community for their versatile applications ranging from green chemistry as media for purification, separation, and catalysis, to bioscience as solvents for biomolecules like proteins or enzymes.[3] In addition, they are considered as realistic candidates to replace the conventional organic carbonate solvents to prepare liquid electrolytes for lithium batteries, due to their low or no toxicity, high thermal stability, low vapour-pressure and flammability. The main drawback for this application is related to their relatively high viscosity, which limits the attainable ionic conductivity. Generally speaking, ionic liquids are organic salts where the cation is based on linear amines, like in the case of quaternary ammonium $[R_4N]^+$, or on cyclic amines, which can be aromatic (pyridinium, imidazolinium) or saturated (pyrrolidinium, piperidinium, morpholinium).[56,57] The anion may be inorganic, as PF_6^-, BF_4^-, halogenide, AsF_6^-, or more frequently organic, like cyanide, perfluoro(alkyl-sulfonyl)imides ($TFSI^-$, $BETI^-$), or perfluoroalkyltrifluoroborates ($[R_FBF_3]^-$). The cation may be easily functionalised with several possible substituents (hydrogen, aliphatic chains, ether based chains, *etc*.) which can properly modulate the physico-chemical properties of the ionic liquids, such as viscosity, melting point, glass transition temperature, surface tension and diffusion coefficients. The nature of the substituents also affects the IL ionicity and, consequently, the salt solubility. For example, the variation in the alkyl chain length causes different balances in the Lewis acid–base interactions of cation and anion and then in their aggregation.[58] Many structures based on both imidazolinium and pyrrolidinium were derivatised by aliphatic lateral chains of different lengths,[57] eventually including heteroatoms like oxygen.[56,59,60] Scheme 2 reports the cation structure of some of the ionic liquids most investigated as potential solvents for electrolytes in lithium batteries.

The group of Passerini reported the role of both linear and branched alkyl side groups on the synthesis and physico-chemical properties of one of the most interesting ionic liquid, namely *N*-alkyl-*N*-methylpyrrolidinium bis(trifluoromethane-sulfonimide) ($PYR_{1A}TFSI$, where A is C_nH_{2n+2} with *n* ranging between 1 and 10).[61] The authors showed that the

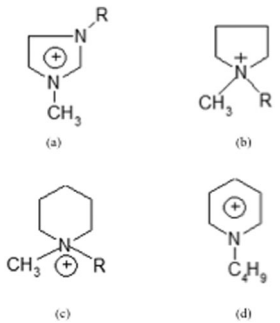

Scheme 2 (a) Alkylimidazolinium; (b) alkylpyrrolidinium; (c) methylalkylpiperidinium; (d) butylpyridinium.

melting point is not affected by the chain length but rather it slightly increases with the branching. The conductivity exceeds 1 mS cm^{-1} at room temperature and generally decreases with the increase of both side chain length and branching, in agreement with the behaviour of the viscosity. Finally, heavier (linear or branched) functional groups do improve the electrochemical stability. Recently, we reported on the preparation and characterization of lithium bis(trifluoromethanesulfonyl)-imide (LiTFSI) solutions in *N*-methoxyethyl-*N*-methylpyrrolidinium bis(trifluoromethanesulfonyl) imide ($PYR_{1,2O1}$-TFSI) ionic liquid.[60] The presence of an ether-based moiety in the side group improves the solubility of the lithium salt. This IL shows a rt viscosity η = 47 cP, which is lower than those typical of pyrrolidinium-based ILs with alkyl units and the same anion (60–90 cP).[57] The ether-based IL is completely amorphous, therefore the conductivity at sub-ambient temperature remains good because of the absence of crystallization phenomena (see Fig. 9).

It was recently shown that some physical and chemical properties, namely viscosity and diffusion coefficients, of ILs may be tailored by preparing blends of ionic liquids with the same cation but different anions. Differences in conductivity and diffusion among the pure systems and the blends were observed by means of NMR correlation techniques. Such an anomalous behaviour was interpreted in terms of possible phenomena of nanoscale segregations and heterogeneities.[62]

Table 1 reports several relevant physico-chemical and electrochemical properties of some of the most interesting ILs for application as electrolytes for lithium batteries. Generally speaking, the pyrrolidinium-based ILs family shows the lowest viscosity values and, consequently, the highest conductivity. It also shows a wide electrochemical window, which can easily reach 6 V, depending on the anion. In this case, the best structure is constituted by a cation with methyl and butyl units as side groups (PYR_{14}), and the anion is TFSI. ILs generally work very well at the cathode, due to their high anodic stability; in contrast, the interface with the Li anode must be improved in order to form more stable passivation layers. The addition of small amounts of additives (5–10 wt%), like PC, may be enough to this aim. It has been recently reported that also the use of $N(FSO_2)^-$ instead of $N(CF_3SO_2)_2^-$ may lead to improvements of the electrode/electrolyte interface.[63]

For what concerns the lithium transport numbers, no remarkable differences are observed with respect to the conventional carbonate-based electrolytes, and rather low

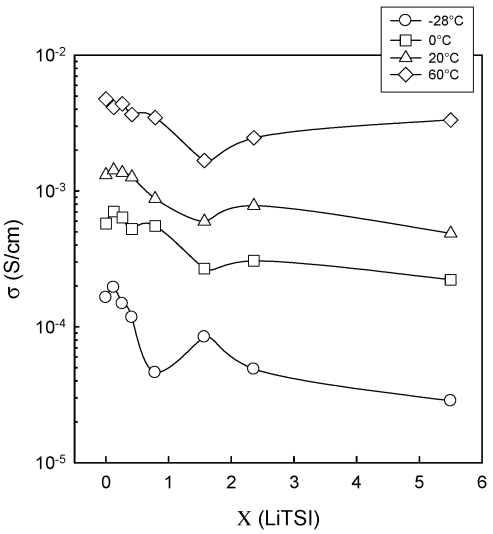

Fig. 9 Conductivity behaviour of the $PY_{1,2O1}$-TFSI–LiTFSI solutions *vs.* the molality, m, measured at different temperatures. T = −28 °C (circles); T = 0 °C (squares); T = 20 °C (triangles); T = 60 °C (diamonds). The lines are guides for the eye. The nonlinear behaviours in the range 0.8–2.5 mol kg^{-1} are likely due to the formation of complexes in the liquid state. Reprinted from ref. 60.

values (about 0.2) are generally reported in the literature,[68] which are not enough for acceptable electrochemical performances. A way to improve the cation transport in ionic liquids was proposed by Ohno and coworkers with the synthesis of zwitterion-based ILs, where both the cation and the anion are covalently bonded at the opposite sides of an organic spacer.[69]

Typical zwitterions consisting of an imidazolinium with different anions showed t^+ of about 0.7. The limiting factor of such systems is that the tethering of the ions increases the melting points and decreases the room temperature conductivity. However, some improvements may be obtained using the $TFSI^-$ ion.

Solid polymer electrolytes (SPEs)

SPEs are ion-conducting single-phase or (nano)composite systems based on polymer–salt complexes. No liquid components, be them an additive, a solvent or a liquid electrolyte, are present. They can be prepared by solvent casting, hot pressing, lamination, extrusion, or even by *in situ* polymerisation. Polyethylene oxide and its copolymers have been explored for many years as suitable matrices for SPEs. PEO is a semicrystalline polymer whose glass transition temperature, T_g, and melting point, T_m, are around −60°C and 65 °C, respectively. Due to its relatively high dielectric constant (ε = 8 in the amorphous phase), it is able to dissolve lithium salts. Several PEO_n–LiX systems were explored in the past, by changing both the molar ratio n = [EO]/[Li], and the anion (X = halide, ClO_4^-, $CF_3SO_3^-$, PF_6^-, $N(CF_3SO_2)_2^-$, BF_4^-, *etc.*).[10] The ion conduction is based on an oxygen-assisted hopping mechanism which takes place in the polymer amorphous phase above its T_g, where long range segmental motion of the chains is allowed. Because of the semi-crystalline nature of the polymer, the conductivity is relatively low at

Table 1 Physico-chemical and electrochemical properties of some ILs relevant for lithium batteries. T_g, glass transition temperature; T_m, melting point; d, η and σ, density, viscosity and conductivity, respectively, measured at 20 °C; EW, electrochemical window

IL	T_g/°C	T_m/°C	d/g cm^{-3}	η/cp	σ/mS cm^{-1}	EW/V	Ref.
$IM_{1,2}$-TFSI	−78	−21	1.52	34	8.8	4.3	64, 65
$PYR_{1,4}$-TFSI	−87	−6	1.39	60	2.6	5.7	61, 66
$PYR_{1,2O1}$-TFSI	−88	—	1.40	48	2.6	5.0	60
$PYP_{1,3}$-TFSI	—	8.7	1.27	59	4.9	5.6	67

room temperature ($\sigma < 10^{-6}$ S cm^{-1}) where the crystalline fraction of the polymer is normally relevant, but it abruptly increases above the melting temperature reaching 1 mS cm^{-1} at 80–90 °C, where all the polymer is in a viscous liquid state. The anion mobility along the polymer chains is normally higher than the cation's one, which is not desirable because it reduces the cation transport number and is a source of electrode deterioration. Low lithium transport numbers ($t^+ < 0.3$) are typically obtained, which may be improved by choosing salts with larger organic anions and huge electron delocalization, like $TFSI^-$, also acting as plasticisers for the polymer, in order to further increase the chain flexibility and then the conductivity.[10,14] Generally speaking, the presence of the salt increases the polymer amorphous fraction, that can reach 100% for n values in the range 8–20, depending on the salt employed.[27] Conductivity values higher than 10^{-5} S cm^{-1} can be obtained in the case of fully amorphous PEO–salt systems. However, the absence of a crystalline phase causes the worsening of the mechanical properties (filmability, dimensional stability, *etc.*). Moreover, the amorphous phases are metastable, and undergo rapid crystallization in a matter of days or weeks, which is accompanied by a strong conductivity decrease. At higher salt contents ($n < 6$), both thermal and spectroscopic techniques highlight the presence of crystalline aggregates which are responsible for the reduction of the conductivity and transport numbers, because of the formation of ion pairs and phase segregation.[70] However, some 6 : 1 crystalline complexes (*e.g.* PEO_6–$LiAsF_6$) may offer unique cylindrical structures where the lithium ions reside without being coordinated by the anions (see Fig. 10).[71] Whereas the ionic conductivity of these complexes is still low, substantial improvements can be obtained by substituting the AsF_6^- ions in the crystal structure with the isovalent $N(CF_3SO_2)_2^-$ ions.[72]

The technological use of PEO–salt SPEs does require an acceptable compromise among the following features: (i) suitable ionic conductivity, (ii) good mechanical properties and (iii) high transport number. Many efforts were made to this aim. One explored way was PEO blending and/or cross-linking with other compatible polymers, such as polyacrylic acid (PAA), polymethylmethacrylate (PMMA), which increase the conductivity and the lithium transport number by blocking the anion. Polystyrene has been often used to give a better dimensional stability to the polyether systems.[10,14] In this case, the physico-chemical properties of the system may be modulated by changing the ratio between the two polymers or other parameters. Gomez *et al.* recently found that the ionic conductivity of poly(styrene-*block*-ethylene oxide) copolymers increases with the molecular weight of the copolymers themselves, due to the increasing presence of inhomogeneous local stresses in the block copolymer microdomains which

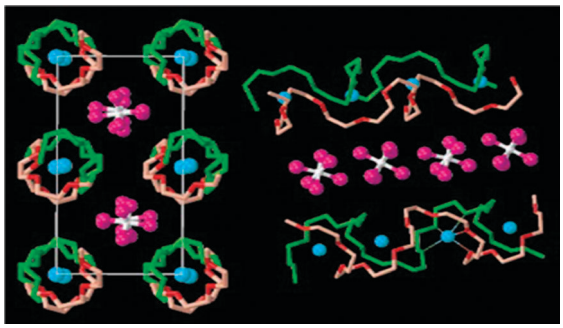

Fig. 10 The structure of PEO_6–$LiAsF_6$ (hydrogen atoms are not shown). Left: view of the structure along the a axis, showing rows of Li^+ ions perpendicular to the page. Blue spheres, lithium; white spheres, arsenic; magenta, fluorine; green, carbon and oxygen in chain 1; pink, carbon in chain 2; red, oxygen in chain 2. Right: view of the structure showing the relative positions of the chains and their conformations. Thin lines indicate coordination around the Li^+ cation. Reprinted from ref. 71.

interferes with the ability of PEO chains to coordinate the Li^+ ions.[73]

The dispersion of ceramic phases (fillers) in PEO-based electrolytes to form (nano)composite systems is perhaps the most effective way to improve thermal, chemical and mechanical stability, and to reduce the tendency to crystallization. Many micro- and nanoscale inorganic oxides[8] were added to the polymer during the film preparation, including insulating SiO_2, Al_2O_3 and TiO_2, superacid conducting zeolites, lithium-based ionic glasses, and, more recently, piezoelectric ceramics like $LiNbO_3$ or $BaTiO_3$.[74] Besides the above-mentioned beneficial effects, the filler may also improve the ionic conductivity. The entity of this effect depends on the filler particles dimensions, which must be below 1 μm, as well as on their microstructure. A recent advance in this field has been given by the use of mesoporous silicas like SBA-15 or MCM-41. It was found that the dispersion of such fillers in PEO–$LiClO_4$ electrolytes leads to conductivity enhancements three times higher than that observed in the case of microsize SiO_2.[75] This improvement is chiefly due to a suppression of the PEO crystalline fraction, as demonstrated by DSC measurements. Nanoscale (and mesoporous) fillers have also a positive effect on both electrochemical stability windows and transport numbers.[8]

Concerning the use of new salts, a few years ago LiBOB has been used to prepare SPEs with PEO, and also nanocomposite systems with Al_2O_3. Ionic conductivity of about 10^{-5} S cm^{-1} was observed at 30 °C.[76,77] More recently, a dual modified composite LiBOB-based SPE was proposed. The modifications were carried out by using calix[6]pyrrole as an anion trap and

nanosize silica as the filler. The most interesting result was $t^+ \approx 0.8$ at 75 °C.[78] Transport numbers close to 0.9 were recently obtained by dissolving a high LiBOB amount ($n = 3$) in block copolymers based on PEO and PMMA. These membranes also showed a wide electrochemical window, exceeding 4.0 V, and good interfacial stability with the lithium anode.[79] A recent advance in this field is the dissolution in several polymer matrices (PEO, polytrimethylene carbonate, and copolymers of acrylonitrile and butyl acrylate) of complex lithium borate salts, namely Li–$[CH_3(OCH_2CH_2)_nO]_3BC_3H_9$, with a number of oxyethylene moieties, n, ranging between 1 and 7. The salt with $n = 3$ shows an interesting conductivity of 2×10^{-5} S cm^{-1} at room temperature. Moreover, the salts with $n \geq 2$ exhibit ionic liquid properties, with glass transition temperatures between −80 and −70 °C. Ionic conductivity of about 10^{-5} S cm^{-1} has been obtained with a 1:1 PEO–salt molar ratio.[80]

Polymers alternative to PEO to fabricate solid polymer electrolytes were developed during the last decade. All these matrices contain ethylene oxide units, including polyethyleneglycol (PEG), polyethyleneoxide-methylether methacrylate (PEOMA) and polyethyleneglycol alkylacrylate, and conductivities similar to those of PEO–salt complexes can be obtained.[10]

Recently, Ohno proposed a new class of solid electrolytes based on polymerised ionic liquids. The SPEs are obtained by proper radical polymerization of ILs.[81] In order to favour only the cation mobility, zwitterionic-like ionic liquids were also considered as polymerizable targets, and new polymerized ionic liquids containing an organoboron unit as the receptor were reported.[82] In the latter case, for LiTFSI equimolar content with respect to the organoboron group, the polymers showed conductivity higher than 3×10^{-5} S cm^{-1} at 50 °C and transport numbers up to 0.87. By means of this approach, the author demonstrated that the ion trapping of some substituents is remarkably more effective in the case of IL-based membranes than for PEO-based electrolytes.

Gel polymer electrolytes (GPEs)

GPEs are formed by swelling a polymer matrix with an electrolyte solution containing proper high-boiling solvents and/or plasticisers. Films with very good free-standing properties and large amounts of absorbed liquid electrolyte may be easily prepared by conventional casting techniques or by phase inversion procedures followed by activation (see below). GPEs are also known as hybrid polymer electrolytes (HPEs), because they combine the cohesive features typical of solid systems with liquid-like transport properties. The typical swelling liquids are polar and non-volatile ones, like phthalates, or linear or cyclic organic carbonates like EC, PC, diethylcarbonate (DEC), dimethylcarbonate (DMC), γ-butyrolactone, *etc*.[9] For what concerns the polymer matrix, several hosts were tested in the past, including PAN, PMMA, polyvinylchloride (PVC) and even PEO.[9,10,14] Indeed, the most important matrix is P(VDF–HFP), which is available with HFP molar contents in the range 5–25%. These materials were firstly proposed as electrolytes for lithium batteries by Bellcore,[83] and are currently the most used in the LPB market.

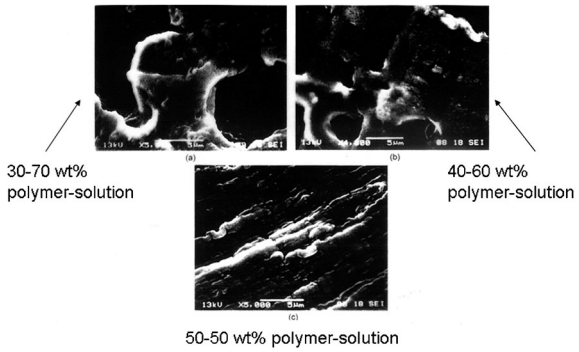

Fig. 11 SEM photographs of P(VDF–HFP) membranes swollen with different amounts of EC/DEC/LiN$(C_2F_5SO_2)_2$ 1 M. Reprinted from ref. 84.

From the point of view of the physical state, GPEs are multiphase systems where crystalline, amorphous/swollen and liquid zones (at least for high electrolyte solution contents) do coexist. Fig. 11 shows the morphology of P(VDF–HFP) membranes swollen with different amounts of EC/DEC/LiN$(C_2F_5SO_2)_2$ 1 M. Liquid cavities are present for solution contents greater than 50 wt%.[84]

The polymer host becomes more amorphous in the swollen state, and its glass transition temperature, T_g, which is generally sub-ambient, further decreases by increasing the liquid content. Contrary to SPEs, the ions move in the liquid or liquid-like phases, and conductivity values near 10^{-3} S cm^{-1} may be obtained at rt in the case of gels with liquid electrolyte/polymer weight ratio higher than 50/50 w/w. For high liquid contents the host matrix simply behaves like an inert or quasi-inert cage, as demonstrated by the behaviour of the longitudinal relaxation rates, T_1^{-1}, measured by ^{7}Li solid-state NMR on PVDF-based gel electrolytes activated by a solution EC/PC/LiTFSI.[85] ^{13}C MAS-NMR also revealed a low level of chemical interactions between the polymer backbone and the nonaqueous electrolyte, at least for liquid concentrations higher than 50 wt%.[85] On the other hand, when substantial amounts of polymer are present, the interactions inside the swollen phase may be relevant, and the microstructure of the swollen polymer affects the carrier migration. The microstructure, in turn, depends on the preparation procedure which is a critical point in the optimization of such membranes.[9,86]

As far as the preparation methods are concerned, conventional casting and the Bellcore technology were in the past the most followed approaches to fabricate free-standing films of PVDF-based copolymers. More recently, phase separation (phase inversion) has been proposed in order to prepare highly porous membranes with controlled and even tunable morphology, which are able to absorb and retain a large amount of liquid electrolyte.[87] The films are prepared as dry samples, and then activated by simple immersion into the electrolyte solution. The solution introduced in the polymer is primarily stored in the pores and then penetrates into the polymer chains to swell the polymer network.

The swelling process and conduction mechanisms of PVDF GPEs prepared by the phase inversion method were investigated by means of NMR self-diffusion coefficients and

ionic conductivity.[88] The dynamics of the swelling process is strongly influenced by the overall membrane porosity, as well as by the pore dimensions. The cation transport number estimated from the NMR diffusion coefficients decreased steeply from ~0.7 to ~0.5 at a porosity of about 70 vol%. It was concluded that the PVDF polymer is effective in enhancing the lithium transport number due to selective interactions with the anion.

Many systems were tested which were based on PVDF homo- and copolymers activated by several types of carbonates and lithium salts. The conductivity values are generally high enough to envisage technological applications in LPB.[9] Good capacity and coulombic efficiency were reported on cells based on GPEs, in the presence of new generation cathodes and anodes.[89]

In spite of these promising results, GPEs suffer from some relevant drawbacks. First of all, in the presence of a large amount of liquid electrolyte, they undergo syneresis with a consequent loss of the overall performances. Furthermore, at a temperature around 50–60 °C, evaporation occurs which also causes a drop in conductivity. Moreover, large quantities of embedded liquid also lead to bad mechanical properties. Some improvements in this sense were obtained by dispersing nanosize inorganic fillers, as in the case of the dry polymer electrolytes.[10] More robust systems in terms of liquid storage were also obtained by preparing gel electrolytes with a nanosponge morphology.[90] However, from the point of view of the commercial use, the most relevant problem is indeed related to the high flammability and high vapor pressure of organic carbonates, which may lead to hazardous explosions in the case of local overheating (thermal runaway).

The most recent approach in the optimization of gel electrolytes is the incorporation of lithium-doped ionic liquids in the polymer host. This approach combines the advantages offered by ILs in terms of non-flammability and safety, with the "quasi-solid" nature of GPEs. The results are non-volatile and thermally stable gels, which can be operated even at high temperatures without polymer degradation and/or decomposition processes. The idea of swelling a polymer with an ionic liquid is not new: already in 1997 Fuller *et al.* proposed P(VDF–HFP) gel electrolytes activated by ethylmethylimidazolinium salts of $(CF_3SO_3)^-$ and BF_4^-.[91] Room temperature ionic conductivity up to 5.8 mS cm^{-1} was obtained, which reached the value of 41 mS cm^{-1} at 205 °C without any system degradation. However, GPEs based on ionic liquids have been systematically investigated only during the last five years, by testing the new IL structures developed in the meantime. In particular, new promising flexible gel electrolytes were prepared by incorporating in PVDF-based polymers alkylpyrrolidinium–TFSI doped with proper amounts of LiTFSI.[10,14,34,92] Scrosati *et al.* chose a lithium solution of the ethylbutyl pyrrolidinium salt to swell P(VDF–HFP) copolymers.[39] The resulting membranes showed conductivity values in the range 0.34–0.94 mS cm^{-1} without undergoing any liquid leakage during a 4 month-long storage. Another advantage of GPEs with ionic liquids is that the host matrix reduces the IL reactivity with respect to Li by forming a protective and quite stable electrode interface (SEI). The interfacial properties may be further improved by adding small amounts of EC and/or PC to the IL solutions, or by dispersing mesoporous fillers in them. Recently, our group has prepared composite gel electrolytes based on PVDF–HFP gelled with a solution of LiTFSI in PYR_{12O1}-TFSI.[34] Two different types of fillers were used, namely a mesoporous silica (SBA-15) and a commercial nanoscale one (HiSil T700™). Both composite gel electrolytes displayed good thermal stability and ionic conductivity. However, the gel electrolytes filled with mesoporous silica showed better electrochemical properties, likely because of a larger polymer/filler interphase, and of the lower number of –OH groups on the filler surface. In particular, lithium transport numbers up to 0.27 and electrochemical windows exceeding 4 V were observed in the membranes with SBA-15 content in the range 5–20 wt%. Fig. 12 compares the cycling behaviours of two solid-state Li/$LiFePO_4$ cells, one based on the GPE filled with the mesoporous silica, and the other one based on the pure IL solution. Only the gel system showed good capacity and cycling properties up to medium C rates (C/5) throughout 180 cycles.

Similar studies have been also carried out with polyethylene oxide. During these last years, several papers described the electrochemical behaviour of PEO-based gel electrolytes, incorporating mostly pyrrolidinium, imidazolinium and piperidinium ionic liquids.[93–95]

Passerini and coworkers prepared and characterised from an electrochemical point of view a ternary system based on PEO–LiTFSI electrolytes gelled with different amounts of *N*-alkyl-*N*-methylpyrrolidinium.[96] As expected, the addition of the IL to the PEO–salt complex increased the conductivity and decreased the interfacial resistance with the lithium anode. Conductivity values higher than 10^{-4} S cm^{-1} were observed at room temperature, about two orders of magnitude higher than those measured for the dry system PEO–LiTFSI. Specific capacity of 100 mA h g^{-1} was obtained at 25 °C with a solid state Li/$LiFePO_4$ cell based on PEO_{10}–LiTFSI-0.96 IL gel electrolyte, where 0.96 represents the PYR_{1A}/Li molar ratio.

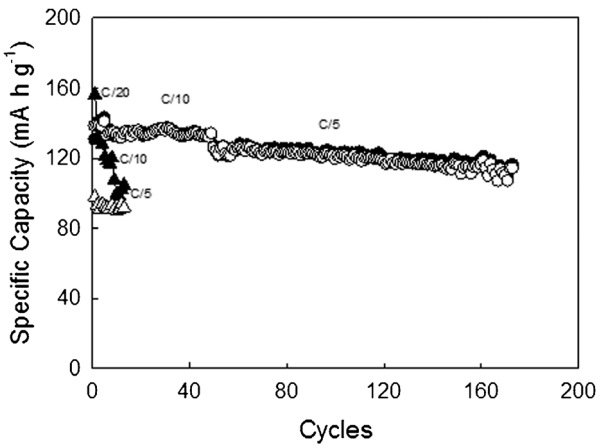

Fig. 12 Cycling behaviour of the Li/$LiFePO_4$ cells based on the ionic liquid electrolyte PYR_{12O1}-TFSI–LiTFSI (m = 0.41 mol kg^{-1}) (open triangle), and on the composite gel electrolyte with 10 wt% of SBA-15 (circles). Open symbols: discharge capacity; filled symbols: charge capacity. 5 wt% of propylene carbonate was added to both the liquid and the gel electrolyte. Reprinted from ref. 34.

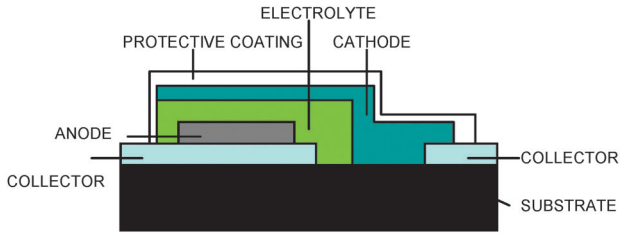

Fig. 13 Scheme of a thin film microbattery.

Recently our group used two ether-functionalised pyrrolidinium ionic liquids ($PYR_{1,201}$-TFSI and $PYR_{1,2(O2)O1}$-TFSI), which differ in ether chain length and oxygen number, as plasticisers for the PEO_{20}–LiTFSI electrolyte.[25] Flexible and homogeneous films were obtained by hot pressing, which showed conductivity approaching 10^{-4} S cm^{-1} at room temperature. However, the electrochemical stability towards Li metal was not good. A relevant problem is that the mechanical strength of ILs containing GPEs based on PEO gets worse at high ionic liquid contents, when the conductivity reaches suitable values. In order to obtain membranes with good dimensional stability and mechanical properties some attempts to cross-link PEO chains were made. Passerini's group again proposed the UV cross-linking of PEO in the presence of the lithium salt and a pyrrolidinium IL at different irradiation times, obtaining a membrane with higher conductivity and improved mechanical properties.[40] However, by comparing several GPEs, Sutto concluded that PVDF-based systems work better than the PEO ones.[97]

Thin film electrolytes for lithium microbatteries

The solid state batteries which use ceramic, glass and glass–ceramic lithium ion conductors (LICs) show, in principle, several advantages with respect to LIB and LPB. These are: (i) better thermally stability, (ii) absence of syneresis or leakage, (iii) safety, even from an environmental point of view, and (iv) wider electrochemical windows. Generally speaking, LICs may be classified into four groups: (i) perovskite-type oxides, *e.g.* (Li,La)TiO_3; (ii) NASICON-structured lithium electrolytes, *e.g.* $LiM^{IV}_2(PO_4)_3$ (M^{IV} = Ti, Zr, Ge); (iii) garnet-type structures containing transition metal oxides, which include $Li_5La_3M_2O_{12}$ (M = transition metal); (iv) glassy and glass–ceramic electrolytes, based on lithium nitrides, sulfides, borates and phosphates. Detailed information may be found in a recent review.[98] These materials generally show a lithium transport number very close to unity, in contrast to the liquid or polymer electrolytes where the anions are mobile. The negligible mobility of non-electroactive ions leads to a high stability of the electrode/electrolyte interface, and electrochemical windows up to 6 V may be often reached, *e.g.* in the case of glassy electrolytes. Unfortunately, but for the perovskite-type systems, which show high ionic conductivity (10^{-3} S cm^{-1}) at room temperature, the lithium ion conductors normally display lower Li conductances (10^{-5}–10^{-6} S cm^{-1} at 20 °C) with respect to the conventional liquid electrolytes. However, this limiting factor may be overcome by the thin film technology. In fact, a 1 μm-thick electrolyte with a conductivity of 10^{-5} S cm^{-1} has a specific resistance of 10 Ω cm^{-2}, which is acceptable for application in the field of lithium microbatteries.[99] At present, the development of microdevices including lithium microbatteries is undergoing a fast and continuous growth, due to the increasing demand on miniaturised systems required by microelectronics, telecommunications, medical implants, military industry and radio-frequency identification (RFID) applications.

A lithium microbattery is made by a high voltage cathode, like V_2O_5, $LiMn_2O_4$, $LiCoO_2$, TiS_2, a LIC thin film as the electrolyte, and an anode which can be made of Li or LiV_2O_5. The observed capacity may reach about 300 mA h g^{-1}.[100] Fig. 13 reports a schematic representation of a thin film microbattery.

Many inorganic materials have been investigated as thin film electrolytes for microbatteries, including several lithium oxides and nonoxides, which differ in crystallinity degree and substituents.[101] The non-oxide systems, *e.g.* Li_3N, Li_2S, Li_2S–SiS_2–P_2S_5, show high ionic conductivity ($\sigma > 10^{-5}$ S cm^{-1}), but their high hygroscopicity is a strong limiting factor.[101,102] In contrast, lithium oxides are more attractive for their stability, although the ionic conductivity is not so high. Typical materials of interest are phosphates, *e.g.* NASICON-structured $LiTi_2(PO_4)_3$[101,103] or Li–P–O, amorphous borates (xLi_2O–B_2O_3) or silicates (Li_2O–V_2O_5–SiO_2).[102,104,105] The ionic conductivity ranges between 10^{-5}–10^{-7} S cm^{-1}, but further enhancements may be obtained by proper substitutions, for instance of P^{5+} with Si^{4+} in the case of phosphates,[102,103] and/or of O^{2-} with N.[99,103] Among the inorganic materials explored during these last years, glassy lithium phosphorus oxynitride (LiPON) still represent the best choice to fabricate thin film electrolytes for lithium microbatteries. LiPON has a phosphate-derived structure, where nitrogen substitutes bridging oxygens of the –PO_4 groups in the glassy network. It was proven that the presence of N atoms remarkably increases the phosphate chemical stability, as well as the film hardness and the devitrification temperature.[106] The main advantage offered by LiPON is its negligible reactivity with the Li anode. The high ionic conductivity of amorphous LiPON is related to the N doping, probably because of the formation of cross-linked NP_3 structures. Improvements of the Li ion mobility were, in fact, observed also in the case of Si-doped Li_2O–P_2O_5 glasses, where the silicon incorporation leads to crosslinked Si–O–P units.[107] Values ranging between 10^{-7} and 10^{-6} S cm^{-1} at 25 °C may be obtained by properly modulating the nitrogen concentration in the glass. LiPON was firstly deposited by Bates *et al.*[107] by means of a radio-frequency (RF) sputtering process, starting from a Li_3PO_4 target in N_2 reactive atmosphere. Many other attempts were successively carried out to deposit thin films of LiPON with different physical techniques, including pulser laser deposition,[108] electron beam evaporation, ion beam processes.[109] However, in spite of the low deposition rates (<3 nm min^{-1}), the sputtering processes seem to offer the best compromise in terms of versatility, economic impact and film quality. The transport properties of the LiPON thin films remarkably depend on the deposition conditions, which also modulate the microstructure and the nitrogen content of the LiPON layers. The highest conductivity value measured was 3.3×10^{-6} S cm^{-1} at 25 °C in the case of films with

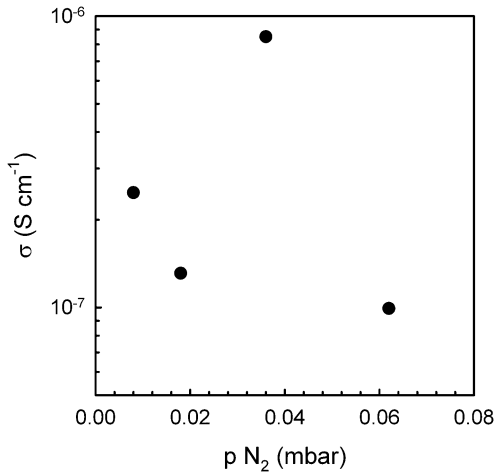

Fig. 14 Conductivity behaviour *vs.* nitrogen pressure for LiPON thin films deposited by means of RF magnetron sputtering (deposition power: 60 W; T = 100 °C). Unpublished results.

composition of $Li_{2.9}PO_{3.3}N_{0.46}$[110] deposited by means of RF magnetron sputtering from a Li_3PO_4 target in N_2/O_2 reactive atmosphere. Generally speaking, the increase of nitrogen pressure, target density and sputtering power seems to improve the ionic conductivity of the films.[111–114] These deposition parameters, in fact, do influence the number of both linear- and crosslinking N bonds replacing the P–O–P ones, which favour the lithium mobility along the glassy structure. However, the dependence of the conductivity on the deposition parameters may be more complex: as an example Fig. 14 shows its behaviour for LiPON thin films deposited by RF magnetron sputtering.

Conductivity values of the order of 10^{-7} S cm^{-1} have been obtained in the explored pressure range, but at 0.04 mbar, where an enhancement of about one order of magnitude has been found. Also the substrate bias voltage may affect the transport properties of LiPON films, by creating local crystalline domains in the glassy structure.[109] However, maxima of conductivity at different N dopings have been reported in the literature. The discrepancy in the results is generally explained in terms of different deposition reactor features, including target–substrate distance, target size, chamber geometry.[114]

E. Towards the future

To date, the LIB and LPB technologies are almost mature, their Technology Readiness Level (TRL) being 9, which means "actual application of the technology in its final form".[115] Therefore, relatively slow improvements must be expected in the near future. As a matter of fact, the USABC roadmap foresees an energy density increase from ~750 to 900 Wh l^{-1} in the next two years for the 18650-type battery, so following a nearly linear trend started in 1992.

Nanomaterials and nanotechnology concepts are expected to play a major role on the battery development, but their impact will likely concentrate on the electrodes, rather than on the electrolyte.[1] Concerning this last component, one of the major challenges will be the search for membranes which are fully compatible with lithium metal, in order to maximize the anode specific capacity. The problem here is to reduce the dendrite formation during battery charge. To this aim, several strategies could be followed, including the use of lithium complexes and of polyelectrolytes,[1] which were earlier tested and abandoned because of their too low conductivity.

A real breakthrough in the LB market can be offered by rechargeable lithium–air batteries (TRL = 3, "active research and development is initiated"). After the initial feasibility demonstration given by Abraham and Jiang,[116] Ogasawara *et al.* showed that the Li_2O_2 formed on discharging may be decomposed to Li and O_2 on charging, with or without a catalyst, and that the charge/discharge cycling may be sustained for many cycles.[117]

Here, the electrolyte development is indeed a critical task. The best results among the conventional organic electrolytes were obtained with PC–THF–$LiPF_6$ which gave a capacity of about 1200 mA h g^{-1} at 0.1 mA cm^{-2} with PVDF-Super P carbon cathodes.[118] Even better performances were obtained with ether-based electrolytes, which allowed capacities higher than 2000 mA h g^{-1}.[119] However, as already stated, these liquids suffer of severe drawbacks, *e.g.* they are flammable, and not hydrophobic. In this frame, ILs are expected to play a major role because of their hydrophobicity, and intrinsic safety. In particular, ILs could contribute to a proper protection of the lithium anode from moisture. On the other hand, ILs display a very high viscosity with respect to standard organic solvents, and proper mixtures with them and salt choices could be considered in order to obtain acceptable conductivity levels.[120] Another key development, here, will be the search for low viscosity cations and, chiefly, anions.[121] Last but not least, it should be considered that ILs are good solvents for ionic materials, and also show high reactivity with metallic lithium. Therefore, multi-layered (ceramic/polymer) or composite electrolytes will be likely needed in order to assure proper shelf-life and cyclability of the (rechargeable) battery.

Finally, the next technological steps will be concerned with the search for more environmentally-sustainable materials and processes, and the waste management and recycling procedures. In particular, lithium availability will rapidly become a strategic item if massive battery use for automotive will be made.

Notes and references

1 M. Armand and J. M. Tarascon, *Nature*, 2008, **451**, 652.
2 Y. K. Sun, S. T. Myung and B. C. Park, *et al.*, *Nat. Mater.*, 2009, **8**, 320.
3 M. Armand, F. Endres and D. R. MacFarlane, *et al.*, *Nat. Mater.*, 2009, **8**, 621.
4 C. P. Grey and N. Duprè, *Chem. Rev.*, 2004, **104**, 4493.
5 M. S. Whittingham, *Chem. Rev.*, 2004, **104**, 4721.
6 M. R. Palacin, *Chem. Soc. Rev.*, 2009, **38**, 2565.
7 D. Jugovic and D. Uskokovic, *J. Power Sources*, 2009, **190**, 538.
8 E. Quartarone, P. Mustarelli and A. Magistris, *Solid State Ionics*, 1998, **110**, 1.
9 A. M. Stephan, *Eur. Polym. J.*, 2006, **42**, 21.
10 J. W. Fergus, *J. Power Sources*, 2010, **195**, 4554.
11 M. M. E. Jacob, E. Hackett and E. P. Giannelis, *J. Mater. Chem.*, 2003, **13**, 1.
12 C. A. Angell, C. Liu and E. Sanchez, *Nature*, 1993, **362**, 137.

13 M. A. Ratner, P. Johansson and D. F. Shriver, *MRS Bull.*, 2000, **45**, 31.
14 R. C. Agrawal and G. P. Pandey, *J. Phys. D: Appl. Phys.*, 2008, **41**, 223001.
15 M. H. Cohen and D. Turnbull, *J. Chem. Phys.*, 1959, **31**, 1164.
16 J. H. Gibbs and E. A. Di Marzio, *J. Chem. Phys.*, 1958, **28**, 373.
17 C. Capiglia, Y. Saito, H. Yamamoto, H. Kageyama and P. Mustarelli, *Electrochim. Acta*, 2000, **45**, 1341.
18 A. Noda, K. Hayamizu and M. Watanabe, *J. Phys. Chem. B*, 2001, **105**, 4603.
19 A. S. Aricò, P. Bruce, B. Scrosati, J.-M. Tarascon and W. Van Schalkwijk, *Nat. Mater.*, 2005, **4**, 366.
20 G. B. Appetecchi, G. Dautzenberg and B. Scrosati, *J. Electrochem. Soc.*, 1996, **143**, 6.
21 G. B. Appetecchi, F. Croce, L. Persi, F. Ronci and B. Scrosati, *Electrochim. Acta*, 2000, **45**, 1481.
22 C. Capiglia, P. Mustarelli, E. Quartarone, C. Tomasi and A. Magistris, *Solid State Ionics*, 1999, **118**, 73.
23 D. A. G. Bruggeman, *Ann. Phys. (Leipzig)*, 1935, **24**, 636.
24 D. S. McLachlan, M. Blaszkiewicz and R. E. Newnham, *J. Am. Ceram. Soc.*, 1990, **73**, 2187.
25 For example, see: E. Abitelli, S. Ferrari, E. Quartarone, P. Mustarelli, A. Magistris, M. Fagnoni, A. Albini and C. Gerbaldi, *Electrochim. Acta*, 2010, **55**, 5478.
26 For example, see: A. Magistris, P. Mustarelli, E. Quartarone and C. Tomasi, *Solid State Ionics*, 2000, **136–137**, 1241.
27 For example, see: P. G. Bruce, M. T. Hardgrave and C. A. Vincent, *Solid State Ionics*, 1992, **53–56**, 1087.
28 P. G. Bruce, J. Evans and C. A. Vincent, *Solid State Ionics*, 1988, **28–30**, 918.
29 K. M. Abraham, Z. Jiang and B. Carroll, *Chem. Mater.*, 1997, **9**, 1978.
30 M. Clericuzio, W. O. Parker, Jr., M. Soprani and M. Andrei, *Solid State Ionics*, 1995, **82**, 179.
31 Y. Saito, C. Capiglia, H. Kataoka, H. Yamamoto, H. Ishikawa and P. Mustarelli, *Solid State Ionics*, 2000, **136–137**, 1161.
32 H. L. Dai and T. A. Zawodzinski, *J. Electrochem. Soc.*, 1996, **143**, L107.
33 J. R. MacDonald, *Impedance Spectroscopy*, Wiley, USA, 1987.
34 S. Ferrari, E. Quartarone, P. Mustarelli, A. Magistris, M. Fagnoni, S. Protti, C. Gerbaldi and A. Spinella, *J. Power Sources*, 2010, **195**, 559.
35 O. Chusid, Y. Gofer, D. Aurbach, M. Watanabe, T. Momma and T. Osaka, *J. Power Sources*, 2001, **97–98**, 632.
36 Y. S. Cohen and D. Aurbach, *Electrochem. Commun.*, 2004, **6**, 536.
37 A. Guerfi, M. Dontigny, Y. Kobayashi, A. Vijh and K. Zaghib, *J. Solid State Electrochem.*, 2009, **13**, 1003.
38 C. Zhao, G. Burrell, A. A. J. Torriero, F. Separovic, N. F. Dunlop, D. R. MacFarlane and A. M. Bond, *J. Phys. Chem. B*, 2008, **112**, 6923.
39 C. Sirisopanaporn, A. Fernicola and B. Scrosati, *J. Power Sources*, 2009, **186**, 490.
40 G. T. Kim, G. B. Appetecchi, M. Carewska, M. Joost, A. Balducci, M. Winter and S. Passerini, *J. Power Sources*, 2010, **195**, 6130.
41 K. Xu, *Chem. Rev.*, 2004, **104**, 4303.
42 P. Arora and Z. Zhang, *Chem. Rev.*, 2004, **104**, 4419.
43 S. S. Zhang, *J. Power Sources*, 2007, **164**, 351.
44 S. S. Zhang, *J. Power Sources*, 2006, **162**, 1379.
45 S. Y. Chen, Z. X. Wang, H. L. Zhao and L. Q. Chen, *Prog. Chem.*, 2009, **21**, 629.
46 G. Park, H. Nakamura, Y. Lee and M. Yoshio, *J. Power Sources*, 2009, **189**, 602.
47 T. Tsujikawa, K. Yabuta, T. Matsushita, T. Matsushima, K. Hayashi and M. Arakawa, *J. Power Sources*, 2009, **189**, 429.
48 D. E. Fenton, J. M. Parker and P. V. Wright, *Polymer*, 1973, **14**, 589.
49 J. Barthel, A. Schmid and H. J. Gores, *J. Electrochem. Soc.*, 2000, **147**, 21, and references therein indicated.
50 Z. M. Xue, W. Zhou, J. Ding and C. H. Chen, *Electrochim. Acta*, 2010, **55**, 5342.
51 W. Xu and C. A. Angell, *Electrochem. Solid-State Lett.*, 2001, **4**, E1.
52 K. Xu, S. Zhang, B. A. Poese and T. R. Jow, *Electrochem. Solid-State Lett.*, 2002, **5**, A259.
53 C. Täubert, M. Fleischhammer, M. Wohlfahrt-Mehrens, U. Wietelmann and T. Buhrmesterb, *J. Electrochem. Soc.*, 2010, **157**, A721.
54 L. F. Li, H. S. Lee, H. Li, X. Q. Yang and X. J. Huang, *Electrochem. Commun.*, 2009, **11**, 2296.
55 C. M. Ionica-Bousquet, D. Munoz-Rojas, W. J. Casteel, R. M. Pearlstein, G. GirishKumar, G. P. Pez and M. Palacin, *J. Power Sources*, 2010, **195**, 1479.
56 Z. B. Zhou, H. Matsumoto and K. Tatsumi, *Chem.–Eur. J.*, 2006, **12**, 2196.
57 M. Galinski, A. Lewandowski and I. Stepniak, *Electrochim. Acta*, 2006, **51**, 5567.
58 K. Ueno, H. Tokuda and M. Watanabe, *Phys. Chem. Chem. Phys.*, 2010, **12**, 1649.
59 L. C. Branco, J. N. Rosa, J. J. Moura Ramos and C. A. M. Afonso, *Chem.–Eur. J.*, 2002, **8**, 3671.
60 S. Ferrari, E. Quartarone, P. Mustarelli, A. Magistris, S. Protti, S. Lazzaroni, M. Fagnoni and A. Albini, *J. Power Sources*, 2009, **194**, 45.
61 G. B. Appetecchi, M. Montanino, D. Zane, M. Carewska, F. Alessandrini and S. Passerini, *Electrochim. Acta*, 2009, **54**, 1325.
62 F. Castiglione, G. Raos, G. B. Appetecchi, M. Montanino, S. Passerini, M. Moreno, A. Famulari and A. Mele, *Phys. Chem. Chem. Phys.*, 2010, **12**, 1784.
63 A. P. Lewandowski, A. F. Hollenkamp, S. W. Donne and A. S. Best, *J. Power Sources*, 2009, **195**, 2029.
64 P. Bonhote, A. P. Dias, N. Papageorgiou, K. K. Alyanasundaram and M. Gratzel, *Inorg. Chem.*, 1996, **35**, 1168.
65 S. V. Dzyuba and R. A. Bartsch, *ChemPhysChem*, 2002, **3**, 161.
66 D. R. MacFarlane, P. Meakin, J. Sun, N. Amini and M. Forsyth, *J. Phys. Chem. B*, 1999, **103**, 4164.
67 T. Yim, H. Y. Lee, Y.-J. Kim, J. Mun, S. Kim, S. M. Oh and Y. G. Kim, *Bull. Korean Chem. Soc.*, 2007, **28**, 1567.
68 J.-H. Shin, W. A. Henderson and S. Passerini, *Electrochem. Commun.*, 2003, **5**, 1016.
69 A. Narita, W. Shibayama, T. Mizumo, N. Matsumi and H. Ohno, *Chem. Commun.*, 2006, 1926.
70 M. Marzantowicz, J. R. Dygas, F. Krok, A. Tomaszewska, G. Z. Zukowska, Z. Florjanczyk and E. Zygadlo-Monikowska, *Electrochim. Acta*, 2010, **55**, 5446.
71 G. S. MacGlashan, Y. G. Andreev and P. G. Bruce, *Nature*, 1999, **398**, 792.
72 A. M. Christie, S. J. Lilley, E. Staunton, Y. G. Andreev and P. G. Bruce, *Nature*, 2005, **433**, 50.
73 E. D. Gomez, A. Panday, E. H. Feng, V. Chen, G. M. Stone, A. M. Minor, C. Kisielowski, K. H. Downing, O. Borodin, G. D. Smith and N. P. Balsara, *Nano Lett.*, 2009, **9**, 1212.
74 Y. Takeda, N. Imanishi and O. Yamamoto, *Electrochemistry*, 2009, **77**, 784.
75 J. Xi, X. Qiu, W. Zhu and X. Tang, *Microporous Mesoporous Mater.*, 2006, **88**, 1.
76 G. B. Appetecchi, D. Zane and B. Scrosati, *J. Electrochem. Soc.*, 2004, **151**, A1369.
77 F. Croce, L. Settimi, B. Scrosati and D. Zane, *J. New Mater. Electrochem. Syst.*, 2006, **9**, 3.
78 H. Mazor, D. Golodnitsky, Y. Rosenberg, E. Peled, W. Wieczorek and B. Scrosati, *Isr. J. Chem.*, 2008, **48**, 259.
79 A. Ghosh, C. Wang and P. Kofinas, *J. Electrochem. Soc.*, 2010, **157**, A846.
80 E. Zygadlo-Monikowska, Z. Florjanczyk, K. Sluzewska, J. Ostrowska, N. Langwald and A. Tomaszewska, *J. Power Sources*, 2010, **195**, 6055.
81 H. Ohno, *Electrochim. Acta*, 2001, **46**, 1407.
82 N. Matsumi, K. Sugai, M. Miyake and H. Ohno, *Macromolecules*, 2006, **39**, 6924.
83 J. M. Tarascon, A. S. Gozdz, C. Schmutz, F. Shokoohi and P. C. Warren, *Solid State Ionics*, 1996, **86–88**, 49.
84 C. Capiglia, Y. Saito, H. Kataoka, T. Kodama, E. Quartarone and P. Mustarelli, *Solid State Ionics*, 2000, **131**, 291.
85 P. Mustarelli, E. Quartarone, C. Capiglia, C. Tomasi and A. Magistris, *J. Chem. Phys.*, 1999, **111**, 3761.

86 E. Quartarone, P. Mustarelli and A. Magistris, *J. Phys. Chem. B*, 2002, **106**, 10828.
87 For example, see: T. Michot, A. Nishimoto and M. Watanabe, *Electrochim. Acta*, 2000, **45**, 1347.
88 Y. Saito, H. Kataoka, E. Quartarone and P. Mustarelli, *J. Phys. Chem. B*, 2002, **106**, 7200.
89 J. Hassoun, S. Panero, P. Reale and B. Scrosati, *Adv. Mater.*, 2009, **21**, 4807.
90 K. S. Liao, T. E. Sutto, E. Andreoli, P. Ajayan, K. A. McGrady and S. A. Curran, *J. Power Sources*, 2010, **195**, 867.
91 J. Fuller, A. C. Breda and R. T. Carlin, *J. Electrochem. Soc.*, 1997, **144**, L67.
92 H. Ye, H. J. Huang, J. J. Xu, A. Khalfan and S. G. Greenbaum, *J. Electrochem. Soc.*, 2007, **154**, A1048.
93 J.-H. Shin, W. A. Henderson and S. Passerini, *Electrochem. Solid-State Lett.*, 2005, **8**, A125.
94 C. Zhu, H. Cheng and Y. Yang, *J. Electrochem. Soc.*, 2008, **155**, A569.
95 J.-W. Choi, G. Cheruvally, Y. H. Kim, J. K. Kim, J. Manuel, P. Raghavan, J.-H. Ahn, K.-W. Kim, H.-J. Ahn, D. S. Choi and C. E. Song, *Solid State Ionics*, 2007, **178**, 1235.
96 G. T. Kim, G. B. Appetecchi, F. Alessandrini and S. Passerini, *J. Power Sources*, 2007, **171**, 861.
97 T. Sutto, *J. Electrochem. Soc.*, 2007, **154**, P101.
98 V. Thangadurai and W. Weppner, *Ionics*, 2006, **12**, 81.
99 J. Schwenzel, V. Thangadurai and W. Weppner, *J. Power Sources*, 2006, **154**, 232.
100 For example, see: S. D. Jones and J. R. Akridge, *Solid State Ionics*, 1996, **86–88**, 1291.
101 J. M. Kim, G. B. Park, K. C. Lee, H. Y. Park, S. C. Nam and S. W. Song, *J. Power Sources*, 2009, **189**, 211.
102 A. Patil, V. Patil, D. W. Shin, J.-W. Choi, D.-S. Paik and S.-J. Yoon, *Mater. Res. Bull.*, 2008, **43**, 1913, and references therein.
103 F. Wu, Y. Liu, R. Chen, S. Chen and G. Wang, *J. Power Sources*, 2009, **189**, 467.
104 N. Kuwata, J. Kawamura, K. Toribami, T. Hattori and N. Sata, *Electrochem. Commun.*, 2004, **6**, 417.
105 N. Kuwata, R. Kumar, K. Toribami, T. Suzuki, T. Hattori and J. Kawamura, *Solid State Ionics*, 2006, **177**, 2827.
106 R. W. Larson and D. E. Day, *J. Non-Cryst. Solids*, 1986, **88**, 97.
107 J. B. Bates, N. J. Dudney, G. R. Gruzalski, R. A. Zuhr, A. Choundhury, C. F. Luck and J. D. Robertson, *Solid State Ionics*, 1992, **53–56**, 647; J. B. Bates, N. J. Dudney, G. R. Gruzalski, R. A. Zuhr, A. Choundhury, C. F. Luck and J. D. Robertson, *J. Power Sources*, 1993, **43–44**, 103.
108 Y. G. Kim and H. N. G. Wadley, *J. Power Sources*, 2009, **187**, 591; Y. G. Kim and H. N. G. Wadley, *J. Vac. Sci. Technol., A*, 2008, **26**, 174.
109 F. Vereda, N. Clay, A. Gerouki, R. B. Goldner, T. Haas and P. Zerigian, *J. Power Sources*, 2000, **89**, 201.
110 X. Yu, J. B. Bates, G. E. Jellison and F. X. Hart, *J. Electrochem. Soc.*, 1997, **144**, 524.
111 Z. Hu, D. Li and K. Xie, *Bull. Mater. Sci.*, 2008, **31**, 681.
112 N.-S. Roh, S.-D. Lee and H.-S. Kwon, *Scr. Mater.*, 2000, **42**, 43.
113 H. Y. Park, S. C. nam, Y. C. Lim, K. G. Choi, K. C. Lee, G. B. Park, S.-R. Lee, H. P. Kim and S. B. Cho, *J. Electroceram.*, 2006, **17**, 1023.
114 Y. Hamon, A. Douard, F. Sabary, C. Marcel, P. Vinatier, B. Pecquenard and A. Levasseur, *Solid State Ionics*, 2006, **177**, 257.
115 *Defense Acquisition Book*, Department of Defence, US, 2006.
116 K. M. Abraham and Z. Jiang, *J. Electrochem. Soc.*, 1996, **143**, N01.
117 T. Ogasawara, A. Debart, M. Holzapfel, P. Novak and P. J. Bruce, *J. Am. Chem. Soc.*, 2006, **128**, 1390.
118 J. Read, *J. Electrochem. Soc.*, 2002, **149**, A1190.
119 J. Read, *J. Electrochem. Soc.*, 2006, **153**, A96.
120 D. Bansal, F. Croce, J. Swank and M. Solomon, in *Molten Salts and Ionic Liquids: Newer the Twain?* ed. M. Gaune-Escard and K. R. Seddon, Wiley, Chichester, UK, 2010, ch. 2.
121 N. Terasawa, S. Tsuzuki, T. Umecky, Y. Saito and H. Matsumoto, *Chem. Commun.*, 2010, **46**, 1730.

